
Solar Sail Structural Analysis via Improved Finite Element Modeling

Proc IMechE Part G:
J Aerospace Engineering
0(0):1–13
©IMechE 2016
Reprints and permission:
sagepub.co.uk/journalsPermissions.nav
DOI:10.1177/0954410016636164
uk.sagepub.com/jaero

Luisa Boni, Giovanni Mengali and Alessandro A. Quarta*

Department of Civil and Industrial Engineering, University of Pisa, I-56122 Pisa, Italy

Abstract

Despite the existence of many studies about the structural analysis of a square solar sail, the need of obtaining reliable numerical results still poses a number of practical issues to be solved. The aim of this paper is to propose a new method that improves the existing analysis techniques. In this sense, the solar sail is modelled using distributed sail-boom connections, and its structural behavior in free flight is studied, using the inertia relief method, at different incidence angles of the incoming solar radiation. The proposed approach is able to circumvent the onset of numerical convergence problems by means of suitable strategies. A non-linear analysis is carried out starting from an initial geometrical configuration in which the whole solar sail is perturbed using a linear combination of the first global buckling modes, obtained with a static eigenvalue analysis. Key points of the procedure are the application of a correct sail pre-stress, a clever choice of the type of elements to be used in the finite element analysis and the use of a suitable mesh refinement. The performance of the new approach have been successfully tested on square solar sails with side length varying from relatively small to medium-large sizes, in the range 10 m - 100 m. A detailed analysis is presented for a reference 20 m × 20 m square solar sail, where the paper shows that the suggested procedure is able to guarantee accurate results without the need of additional stabilization technique. In particular, the vibration global mode shapes and frequencies of the solar sail are correctly described even in presence of unsymmetrical loading conditions. In other terms, the numerical analysis is completed without any convergence problem and any disturbing local modes.

Keywords

Square solar sail, solar sail structural analysis

Nomenclature

E, G = elastic moduli, [Pa]
 α = incidence (cone) angle, [deg]
 δ = clock angle, [deg]

* Corresponding author; e-mail: a.quarta@ing.unipi.it

ν = Poisson's ratio

1. Introduction

The recent successes of the Japanese probe Interplanetary Kite-craft Accelerated by Radiation Of the Sun (IKAROS) ^{1,2,3} and of the American NanoSail-D2 ^{4,5,6}, have shown the effectiveness of the concept of a photonic solar sail as a space propulsion system means and confirmed the feasibility of deploying a large gossamer structure both in a low-Earth orbit (NanoSail-D2) and in the interplanetary space (IKAROS). The advances in the manufacturing technology of macro-elements that constitute a solar sail, such as the large reflecting film and the complex structure necessary for sail stiffening and deployment, have only recently impressed a marked acceleration to the actual realization of solar sail-based missions ⁷. In this context, the launch from the Planetary Society of the LightSail-1 solar sail, which is scheduled to take place in the next 2016 ⁸, will represent another step forward in the use of this advanced (and exotic) propulsion system, since a large solar sail, with an area of 32 m², and a reflecting surface in Mylar is going to be deployed in a low-Earth orbit.

After a period along which the scientific community has been mainly concentrated in analyzing mission scenarios ⁹ where the concept of a photonic solar sail was shown to be a competitive option compared to other and more conventional propulsion systems ^{10,11,12,13}, recently the focus is being shifted toward purely engineering problems (mainly related to structures and systems) for the realization of solar sail-based spacecraft. The latter aspect is clearly proved from the last (i.e., third) International Symposium on Solar Sailing ¹⁴ of 2013, in which the papers involving "technology activities" for solar sails are about a quarter of the total number. The interest for a practical realization of a solar sail is also drawn by many academic projects that are going to accomplish scale models of these propulsion systems ^{15,16,17,18}.

From a structural viewpoint, the analysis of a complex space structure such as a solar sail makes large use of commercial techniques and softwares, which are commonly used in the design of more conventional aeronautical and mechanical structures. Even though the modern software packages for Finite Element Analysis (FEA) represent essential tools for the preliminary design of aerospace structures, the peculiarity of a solar sail structure, such as the wide reflecting surface with a very small thickness and the long and slender stiffening booms, gives rise to a number of challenging problems both in the modeling and in the analysis phase.

Not surprisingly, as far as square solar sails are concerned, the literature reports a number of papers dealing with different kinds of static and dynamic structural analyses as a function of the sail's side length. The interest for this kind of problem can be traced back to the exhaustive paper by Greschik and Mikulas ¹⁹, in which the design parameters of a square solar sail are shown to be very complex to manage in a comprehensive (and closed-form) way using analytical methods only. In this context, Murphy et al. ²⁰ discuss one of the first attempts of using a finite elements method approach to perform a dynamic structural analysis of a square solar sail. However, in Ref. [20] no detail is provided in terms of software used and type of eigensolver chosen, nothing is said about the loads and constraints applied, nor about the type of elements adopted. Nevertheless, several problems of convergence are pointed out ²⁰, due to the presence of sail membrane zones in compression, which cause the occurrence of wrinkling phenomena on the sail surface. The presence of such regions also induces undesired chatter modes, consistent with local deformation patterns. In Ref. [20] this problem is eventually circumvented by applying a pre-load, which produces a stress of about 1.5 Pa at the center of the sail quadrants, but no information is provided about the pre-stressing method, and the first mode shape only (with its corresponding frequency) is obtained.

In other papers, dating back to the same period, the interest is focused on the problem of the occurrence of wrinkling phenomena in the regions of the sail membranes subjected to compression, rather than on the global structural response of the solar sail. In Ref. [21] the membrane elements are shown to be unable to reveal the sail zones subjected to wrinkling, whereas the performance of shell elements are investigated with simple square membranes, loaded in traction at the four vertices. The 500 mm \times 500 mm Kapton membranes are analyzed with special four-node, shear-deformable shell elements (S4R5), available in the commercial package ABAQUS. The geometrically non-linearly post-wrinkling analysis is carried out by introducing initial geometrical imperfections obtained from a previous eigenvalue analysis and by using an automated pseudo-dynamic stabilizing function. In Ref. [22] the authors present a method to investigate the formation and evolution, during the loading process, of wrinkling phenomena in a partially wrinkled structure, using buckling and post-buckling solutions with the GENOA code.

Sleight and Muheim²³ report remarkable improvements in the study of a whole square solar sail whose numerical model consists of a free-flying structure in the space environment. The main contribution of that paper²³ is in the use of the inertia relief method, which allows the externally applied solar pressure load to be balanced with inertial loads induced by a constant rigid body acceleration field. Basically, the structure is assumed to be in a state of static equilibrium without constraints. Accordingly, it can be analyzed by means of a classic static analysis. Such a technique, which is extensively discussed in Ref. [24], is available both in NASTRAN and ABAQUS softwares and represents an important tool, useful for avoiding an excessively conservative structural design of the solar sail. In particular, Greschik and Mikulas¹⁹ show that ignoring the inertial effects due to the sail's acceleration, may induce boom deformations up to three times greater than those due to the flight condition. The main problem of the inertia relief method consists in its total incompatibility with any type of stabilization analysis. This is possibly the main reason why such a powerful technique has no longer used in the succeeding literature works.

As a matter of fact, after Ref. [23], the inertia relief method specifically applied to solar sails can be found only in a recent work by Potes²⁵. However, Ref. [23] use membrane elements and assume a pre-tensioning pattern which is unable to avoid large sail regions in compression. As a result, in the extraction of the vibration mode shapes and frequencies, the first mode only is found numerically. Furthermore, in the parametric study performed on the sail side ranging from 20 m to 150 m, the payload mass at the end of the control mast and the instrumentation mass at the center of the space bus are simply kept constant to the values of 228 kg and 55 kg respectively for each sail size. As far as the smaller solar sail is concerned, those oversized masses can determine unrealistic vibration mode shapes and frequencies that follow unsymmetrical patterns. Also, it is not clear how the viscous stabilization, declared to be used in the paper, is implemented together with the inertia relief method, as the two analysis options are not mutually compatible²⁶.

Taleghani et al.²⁷, with the aid of NASTRAN, perform a statical analysis of a simple triangular sail sector with a 10 m edge without a reinforcing structure and under a constrained status. Shell elements are used, also in the succeeding dynamic analysis, but no information is given on the strategies adopted for the convergence and on the procedures for load application. Likewise in Ref. [28], where similar studies are extended to a 20 m \times 20 m square solar sail without control mast, no clarification is offered about the FEA strategies.

An interesting comparison between the performance of the two software packages NASTRAN and ABAQUS is available in Ref. [29], where a 10 m \times 10 m square solar sail is analyzed both statically and dynamically. After pre-tensioning, instead of using a distributed surface load, the force associated to the solar radiation pressure is simulated with concentrated forces on the booms. This simplification makes the convergence easier, but prevents the correct description of the strain state of the sail membranes, as is shown by comparing the numerical results with experimental data. Membrane elements and viscous stabilization are used in the ABAQUS model, whereas

a shell model with NASTRAN fails the convergence and is replaced by an isogrid model with bar elements for simulating the sail membranes. In the dynamic analysis three vibration modes are extracted, but only the first mode shape is shown.

In Ref. [30] a combined structural-thermal analysis is performed with NASTRAN on a single sector of a $20\text{ m} \times 20\text{ m}$ square solar sail, and the effects of a non-uniform temperature field on the structural response of the sail are studied. The reinforcing booms are not accounted for, 3-node shell elements are used and a constrained structure is assumed. The influence of a non-zero inclination angle of the solar pressure on the thermal field is also discussed. In Ref. [31], a square solar sail sector of 80 m side, constrained at the four vertices, is analyzed by means of an user-defined FEA code. The simplified model is set up with special membrane elements, but no comparison is given with any element provided by commercial software.

Despite the remarkable improvements of FEA software performance during the last years, the techniques used to carry out a structural analysis of a solar sail have not much changed. A significant example is given by Holland³² who, among several types of structural analysis on solar sail components, performs a FEA of a square solar sail using NASTRAN, pointing out serious problems of convergence. In fact, the use of a sail pre-tensioning is unable to avoid the occurrence of wrinkling phenomena. To achieve convergence, Holland³² applies small out-of-plane forces in a quasi random manner, to force the model to a feasible static configuration. In this case the use of a shell model is then dropped to perform a dynamic analysis, the latter being carried out with a model in which the sail is replaced by a network of wires.

The convergence question for a solar sail non-linear analysis, especially for a square configuration, still represents a challenging problem. The strong non-linear behavior of the structure is mainly related to the structural coupling of extremely thin sail membranes with very long and slender reinforcing booms. This problem is amplified by the difficulty of modeling the solar sail structure in presence of distributed sail-boom connections. Furthermore, due to the negligible bending stiffness of the sail membranes, the transition from in-plane to out-of-plane stress-strain field is a numerically highly unstable issue, which gives rise to a temporary rigid-body motion. Such an obstacle is usually countered by reducing the structure complexity, that is, by using simplified sub-components, assuming unrealistic constraints and loading conditions, or introducing stabilization methods of various types. These tricks, however, cause the occurrence of inaccuracies in the numerical results. Moreover, the introduction of stabilization methods can invalidate the use of the inertia relief technique, which is essential for representing realistic in-flight conditions.

The aim of this paper is to improve the existing analysis techniques to obtain reliable numerical results. A FEA procedure has been developed and its effectiveness has been tested on square solar sails whose side ranges from 10 m to 100 m. In the proposed approach, the whole square solar sail structure is studied in presence of distributed sail-boom connections. The inertia relief method is adopted to analyze the sail behavior in a free-flight condition as a function of the incidence angle of the solar flux. Such an analysis procedure allows the stress and strain state of both the sail membranes and the reinforcing booms to be evaluated, and the solar sail vibration frequencies to be identified under realistic loading conditions. More precisely, the structural response of the solar sail is analyzed with a FEA method, using the commercial package ABAQUS V 6.11³³. The main contribution of this paper consists in the discussion on how the classical numerical convergence problems can be avoided. In particular, a non-linear analysis is performed on an initial geometrical configuration of the whole solar sail, perturbed with a linear combination of the first four global buckling modes, the latter being obtained by means of an eigenvalues analysis. Such a technique, which is known to be effective in performing non-linear post-buckling analysis of aerospace structural components (see Ref. [34]), is used in Ref. [21] on small-scale models to study the post-wrinkling behaviour of $500\text{ mm} \times 500\text{ mm}$ Kapton membranes. In that paper²¹, however, the post wrinkling behavior is studied by means of *local* instability patterns. Here, instead, the use

of *global* instability modes is shown to be an effective means for improving the algorithm convergence even when large side configurations are accounted for. The linear buckling analysis is conducted taking into account the actual pre-stress and surface load, so that the initial geometrical imperfection has the double beneficial effect of improving the numerical convergence and driving the non-linear solution algorithm towards realistic deformed configurations. To preserve the accuracy of the results, the amplitude of the geometrical imperfection is chosen to be at least two order of magnitude smaller than the maximum sail deflection. Other key points are represented by the use of a proper sail pre-stress, the choice of a suitable element type for the FEA and the employment of a sufficient mesh refinement. As long as the sail side is sufficiently small, usually it is not difficult to obtain reasonable results without the need of any stabilization technique. On the contrary, the use of an initial geometrical imperfection becomes mandatory, especially as far as solar sail of large size are concerned, to avoid the need of artificial stabilization methods and to improve the convergence performance. Also, the solution accuracy and the convergence performance are further improved by replacing the classical symmetric eigensolvers with unsymmetrical ones, used for both the buckling and the frequency analysis, in presence of unsymmetrical loading conditions. A description of the methodology adopted and the results of the FE analysis are now discussed for a reference configuration of a $20\text{ m} \times 20\text{ m}$ square solar sail. It is assumed that the sail loading parameter, defined as the mass per unit area of the whole spacecraft, is about 0.18 kg/m^2 . The value of the total mass of the spacecraft, as is discussed in the following section, accounts for the masses used for attitude maneuvers, as well as for the mass of payload, instrumentation and other devices. The loading conditions associated to the masses used for attitude maneuvers are not considered in this study.

2. Solar sail architecture

The solar sail architecture is shown in Fig. 1. It is a square $20\text{ m} \times 20\text{ m}$ solar sail, whose numerical model is built entirely, that is, without assuming any geometrical symmetry, to better capture the structural response of the spacecraft. Following Greschik and Mikulas¹⁹, two different sail configurations have been investigated: the first one, referred to as Five Points Connected Sail (5PCS), see Fig. 1(a), is characterized by four separate triangular sectors, connected to four booms at five points. In the second configuration instead, referred to as Multiple Points Connected Sail (MPCS), see Fig. 1(b), the four sail sectors are connected to the booms at multiple points.

The sail sectors, each one of about 15 m length, are attached to the booms by means of a variable number of cables, depending on the spacecraft configuration. In the MPCS, the inner cable spacing has been selected on the basis of a compromise solution between the simulation of connections in a nearly continuous way¹⁹ and an acceptable computational effort, the latter being closely related to the convergence performance. In the solar sail architecture, a 2 m control mast (i.e., a thin-walled pipe directed along the normal axis from the hub) is also considered, with a concentrated mass of about 35 kg at the end. The selected control mast sizing is characterized by a high stiffness, such as to guarantee an absence of interference with the fundamental modes of the sail system. Furthermore, four concentrated masses of 0.6 kg each, which model four tip plates, are placed at the end of each boom. Finally, a concentrated mass of 25 kg is at the central spacecraft bus, accounting for instrumentation, gimbals, fittings and other devices.

Each component of the spacecraft is modeled using classic materials for a square sail structure^{23,35,36}. The sail membranes are made of isotropic material with properties similar to Kapton, the booms are of composite material and the cables of isotropic material similar to Kevlar, whereas the material for the control mast is assumed to be isotropic. The material properties are summarized in Table 1, where the density of the membrane

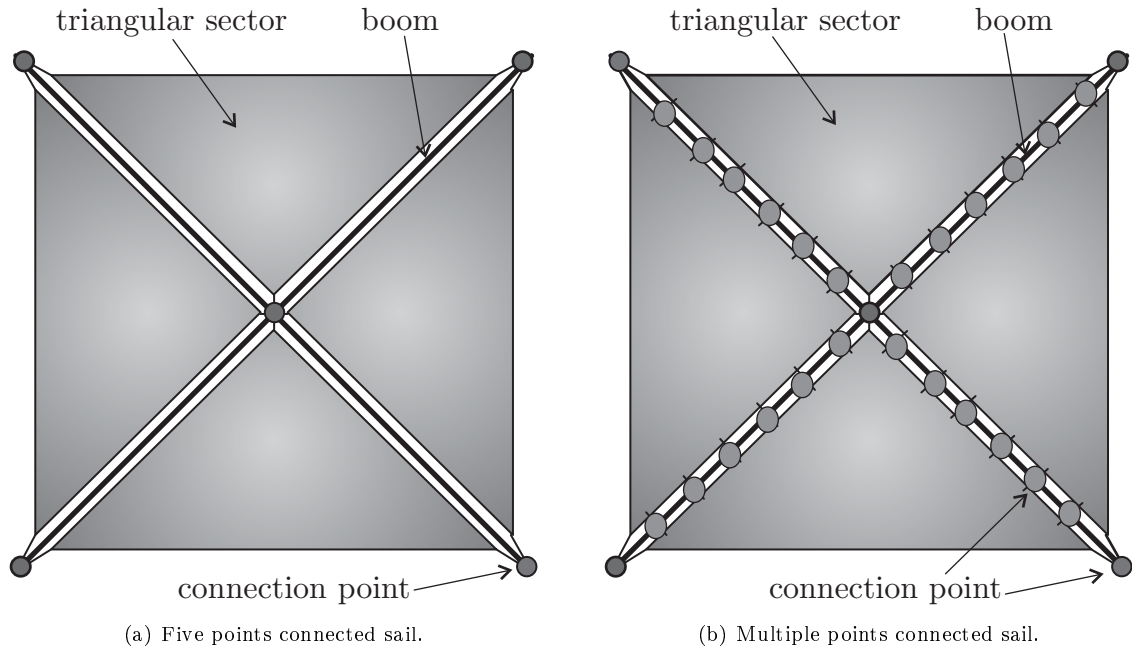


Figure 1. Square solar sail models (adapted from Refs. [19, 23]).

sail material accounts for the presence of film, coating and bonding substrate. The total mass of the two configurations is about 72 kg each.

3. Analysis strategies

The developed FEA takes into account the geometrical non-linear behavior of the model by means of a classic non-linear analysis based on a Newton–Raphson algorithm, without the need of any non-zero stabilization parameter. The non-linear analysis is performed on an initial geometrical configuration perturbed with a linear combination of the first four global buckling modes, given by a previous eigenvalues analysis. In the special case of a sail size of 20 m, the first four modes are all of global type, being the occurrence of local modes promoted by the increase in the size of the sail side, rather than by the increase in the number of the inner connecting

Component	Boom	Cable	Control mast	Sail membrane
Material	composite	isotropic (Kevlar type)	isotropic	isotropic (Kapton type)
Section shape, radius [m]	tube circular, 0.229	solid circular, 0.0005	tube circular, 0.01705	N/A
Thickness [m]	7.5×10^{-6}	N/A	0.005	2.5×10^{-6}
Density [kg/m^3]	1908	1440	7660	1572
Elastic moduli [Pa]	$E_1 = 124 \times 10^9$	62×10^9	124×10^9	2.48×10^9
	$E_2 = 100 \times 10^9$			
	$E_3 = 100 \times 10^9$			
	$G_{12} = 47 \times 10^9$			
	$G_{13} = 38 \times 10^9$			
Poisson's ratio	$\nu_{12} = 0.3$	0.36	0.3	0.34
	$\nu_{13} = 0.3$			
	$\nu_{23} = 0.3$			

Table 1. Geometry and material properties of the solar sail components.

cables. For this reference configuration, the selected amplitude for the geometrical imperfection is 0.1 mm. A multi-step approach has been used for analyzing the two sail configurations. First the sail membranes have been pre-stressed. Then, an uniform surface load, which simulates the force induced by the solar radiation pressure, has been applied to the sail surface. Finally, the vibrations frequencies of the spacecraft have been calculated.

The inertia relief method has been used in this study. A conventional static analysis assumes that in strain free conditions the model cannot move as a rigid body. In such a case, the stiffness matrix of the model becomes singular and, when the FE solver attempts to decompose it, a fatal message occurs or unreasonable answers are obtained. In this context, the “inertia relief” is an advanced option, implemented within ABAQUS software ³³, that allows unconstrained structures to be simulated in a static analysis, by using the inertia of the structure to resist the applied loadings. In that way, the assumption is made that the structure is in a state of static equilibrium even though it is not constrained. To invoke this option, a list of six non-redundant degrees of freedom that describe the possible unconstrained motion must be provided, then the solver calculates the forces that result from a rigid body acceleration. The latter is obtained such that the inertial forces balance perfectly the external applied forces. The solver, on the basis of the mass distribution of the structure, selects a reference point, generally coincident with the center of mass of the structure, which must be constrained to a zero displacement in the directions of the specified degrees of freedom. The solver provides the relative motion of all other grid points with respect to the reference point. At the end of each inertia relief analysis the constraint forces at the reference point must be nearly equal to zero, to guarantee the correctness of the approach. Such a criterion has been met for all of the simulations performed in the analysis.

Two load distribution cases have been considered for each sail configuration: a normal pressure of modulus $9.12 \times 10^{-6} \text{ N/m}^2$, corresponding to the solar pressure exerted at 1 au, and a surface load with an incidence (cone) angle $\alpha = 35 \text{ deg}$ with respect to the sail’s normal, which maximizes the tangential force on the sail nominal plane during the spacecraft orbital motion around the Sun ⁹. In this last case, the surface load direction has also been applied with a clock angle, in the sail nominal plane, of $\delta = 45 \text{ deg}$ with respect to the solar sail horizontal axis ³⁰.

3.1. Finite Element Models

As far as the sail membrane is concerned, the model developed uses a mesh dominated by 4-node doubly curved shell S4 elements. This kind of shell element is able to capture the slightest bending stress that can affect the sail during the loading phases and to deal with sail areas in compression and subjected to possible wrinkling phenomena. Alternative choices of shell elements have important deficiencies. For example, even though S4R elements with reduced integration could probably reduce the required computational time, they are subjected to serious problem of hourglassing, especially near zones of stress concentration, such as the cable-boom and cable-sail connections.

Due to the triangular shape of the sail sectors, a small amount of S3 shell elements with three nodes is present in the mesh, about 1500 in a model of 15000 elements. As is discussed in Ref. [33], the S3 elements, which are commonly used in the literature for triangular solar sail sectors, provide accurate results in most loading situations. However, because of their constant bending and membrane strain approximations, a very high mesh refinement is often required to accurately model the bending deformations or to find solutions to problems involving high strain gradients, which can occur in the analyzed cases.

Furthermore, the use of 4-node elements induces a regularity of the mesh that allows the extraction of outputs on linear paths to be obtained, or the definition of a regular boundary for a possible sub-model, to be used in succeeding detail analysis. The supporting booms and the control mast are modeled with B31 beam elements, while the cables with T3D2 truss elements. Mass points have been used for all of the concentrated masses. A

structured meshing technique has been used for each part of the FE models. Figure 2 shows the mesh of the two models along with the main components of the square solar sail. In particular, the model for the MPCS model has been obtained from the 5PCS model by adding inner cables every 1.75 m.

The cables have been connected to the boom and to the sail sectors by means of connectors with a section of basic translational type (joint). The pre-tensioning of the cables has been realized by means of a predefined initial field of stress, applied on the truss elements, of about 19 N for each cable in the 5PCS model and of 13 N in the MPCS model.

The pre-tensioning load has been selected such that the stress in the central part of each sail sector is about 1 Psi. A sufficient pre-tensioning level is fundamental, especially for the 5PCS model, to circumvent convergence problems during the processing phase and to avoid the presence of large sail areas in compression, which correspond to possible detrimental wrinkled sail zones. In the last step of the FEA, the first five vibration mode shapes and associated frequencies have been obtained using the Lanczos eigensolver in the non-default unsymmetrical form.

4. Simulation Results

The FE analyses have been performed using a HP Z600 Workstation with eight Processors Intel Xeon X5550 QC 2.66 GHz and 32 Gb of RAM. The computational time is about three minutes for the 5PCS configuration analyses and five minutes for the simulation of a MPCS configuration. An automatic time increase has been adopted for both the pre-stress step and the surface load step, with a typical initial increase of 0.1.

4.1. Effect of the pre-stress load

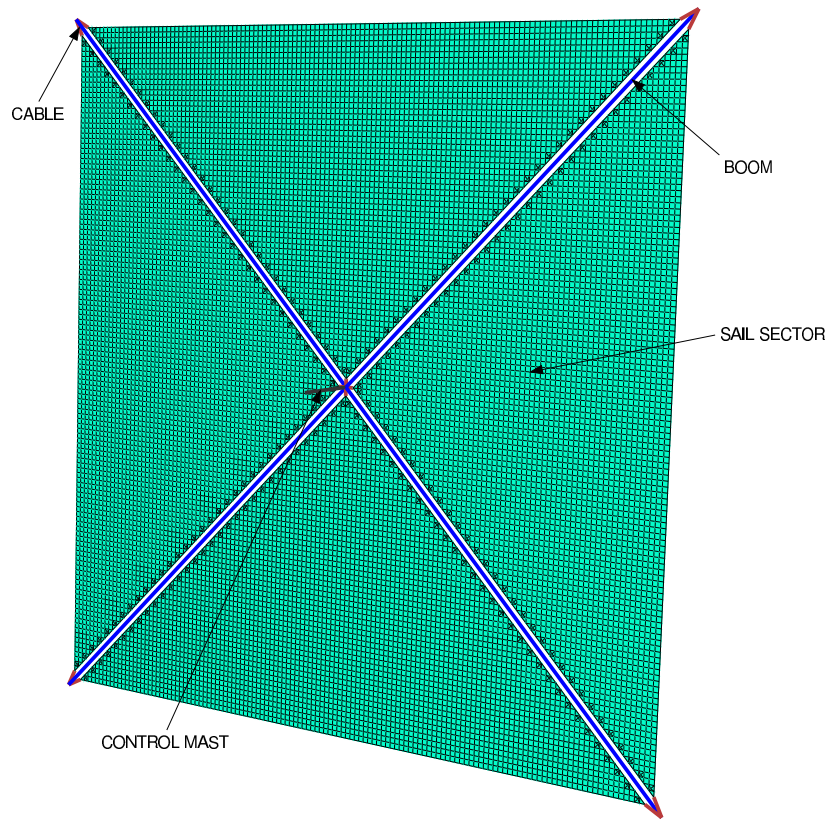
The stress state of the solar sail for the two configurations is illustrated in Fig. 3, where it is shown that the Von Mises stress at the center of each solar sector is about 1 Psi or 6895 Pa. Actually, as is shown in Fig. 3, the applied constant pre-tensioning of the cables causes a qualitatively different stress fields on the sail sectors for the two analyzed configurations: in the 5PCS case the less stressed regions are placed at the sail free edges, while in the MPCS such zones move towards the inner vertex, at the center of the structure. The stress distribution after pre-stress strongly affects the structural response of the solar sail to the pressure load from the solar flux, both in terms of sail maximum deflection and for presence of wrinkled zones, as is discussed in the next section.

4.2. Effects of the surface load

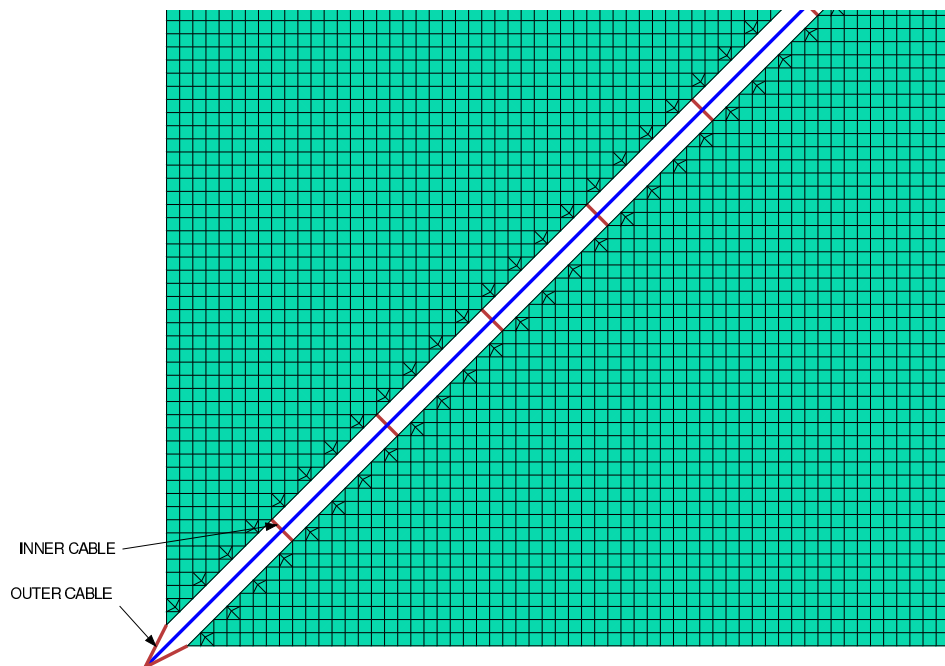
The surface load simulating the force due to the solar radiation pressure induces a significant out-of-plane displacement field on the sail surface, which reaches the maximum value at the center of the external edge of each sail sector, as is shown in Fig. 4.

The normal pressure applied to the sail surface results in a perfectly symmetrical out-of plane displacement field, while the presence of a cone angle α and a clock angle δ , produces an unsymmetrical field. Table 2 reports the maximum deflection of the solar sail for each configuration and load case. The point of maximum out-of-plane displacement is always at the center of a free sail edge, but the edge varies with the load case.

According to the values of Table 2, the different type of connections between sail edges and booms for the two sail configurations cause different deformation effects. In particular, the MPCS model is characterized by a significantly lower maximum deflection with respect to the 5PCS model. As far as the sail edge (with a 20 m length) is concerned, the decrease of the value of the sail maximum deflection introduced by the MPCS when compared to the 5PCS is of about 36%. Such a result points out how a distributed connection between sail membrane and boom can provide not negligible improvements even for a small size solar, which contrasts with

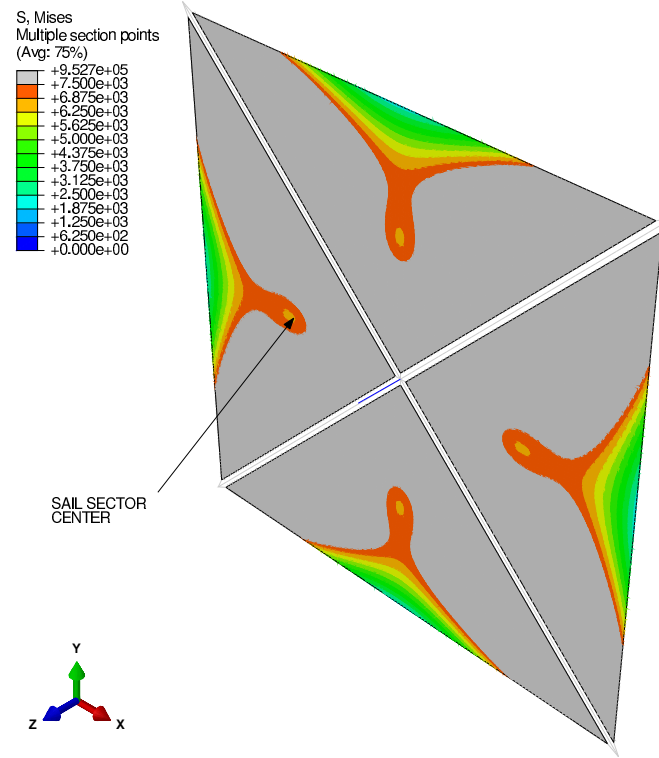


(a) 5PCS: mesh and components.

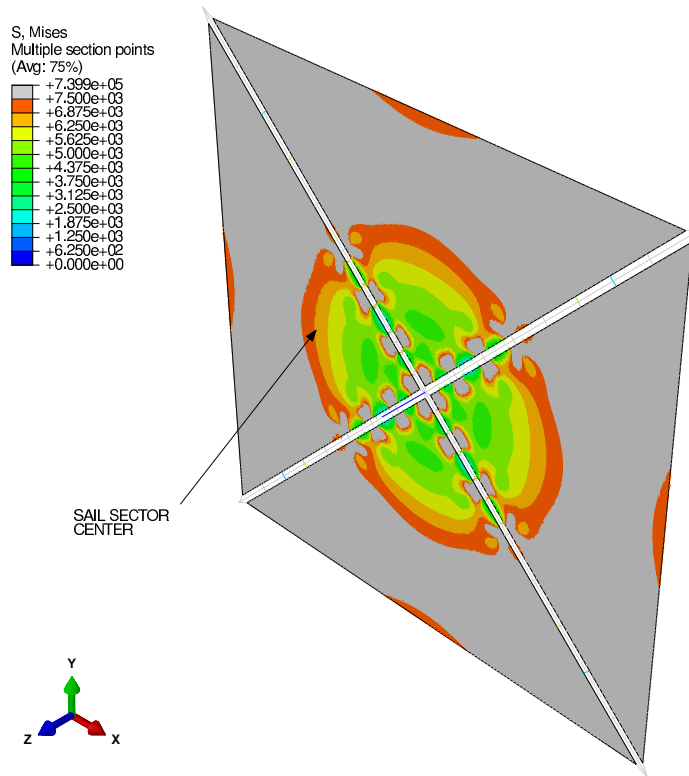


(b) MPCS: detail of mesh.

Figure 2. Mesh of the square solar sail.

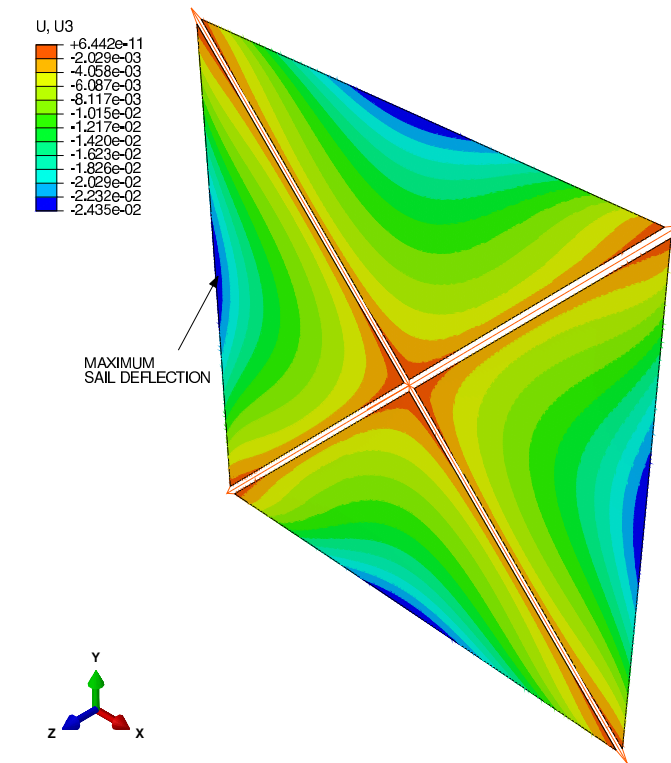


(a) 5PCS.

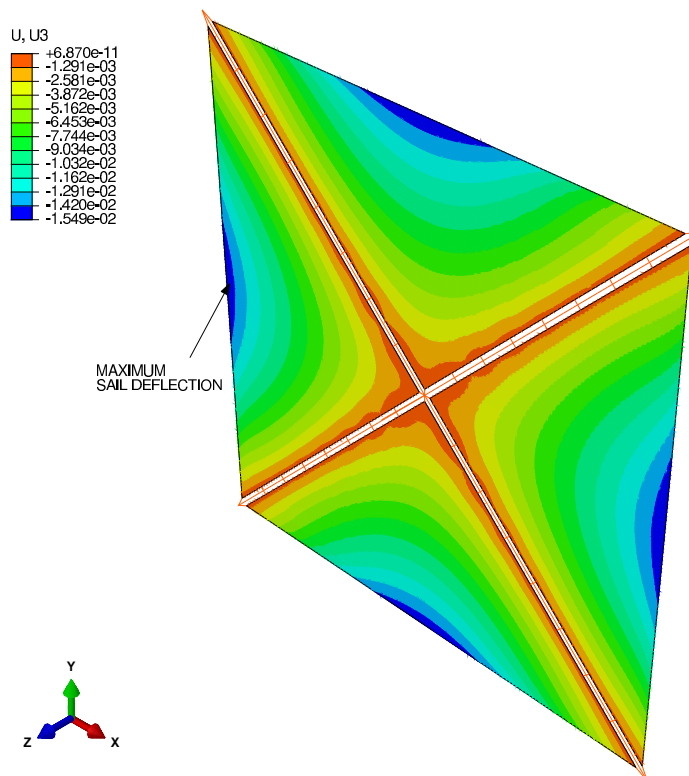


(b) MPCS.

Figure 3. Stress state due to pre-load.



(a) 5PCS.



(b) MPCS.

Figure 4. Out-of-plane displacement.

Model	Angles					
	α	δ	α	δ	α	δ
	0	0	35 deg	0	35 deg	45 deg
5PCS	0.02435 m		0.02139 m		0.02125 m	
MPCS	0.01549 m		0.01387 m		0.01376 m	

Table 2. Maximum sail deflection as a function of the cone (α) and clock (δ) angle.

Model	Angles					
	α	δ	α	δ	α	δ
	0	0	35 deg	0	35 deg	45 deg
5PCS	1.684×10^{-5} m		1.6×10^{-5} m		1.647×10^{-5} m	
MPCS	1.488×10^{-5} m		1.368×10^{-5} m		1.42×10^{-5} m	

Table 3. Maximum boom deflection as a function of the cone (α) and clock (δ) angle.

results of Ref. [23], where the differences between the two configurations become appreciable only starting from a 70 m sail length. Notably, the introduction of a cone angle different from zero does not introduce significant differences in the maximum value of the sail out-of-plane displacement.

The load on the sail surface causes the presence of some regions in compression, which can originate detrimental wrinkled zones. A suitable pre-tensioning of the sail membrane should avoid an excessive extension of such areas. The minimum principal stress field on the sail sectors provides a map of the regions that can be subjected to wrinkling phenomenon. From Fig. 5, which shows the minimum principal stress for the two considered configurations, it is evident the remarkable reduction of compressed zones in the MPCS model, when compared to the 5PCS model, in presence of a pre-stress pattern constant on the cables. In particular, the minimum principal stress field is shown for both the bottom and top faces of the sail (with respect to the sail's normal direction). Even though the difference between the two faces is small, it highlights the presence of a sail bending, which can affect the pattern of wrinkled regions. Such a bending effect would be a-priori neglected by imposing a pure membrane behavior of the sail. Figure 5 only illustrates the results due to the normal pressure, since those corresponding to non-zero load incidence angles are very similar.

The structural response of the supporting booms have been studied in terms of maximum deflection and maximum compressive load. Tables 3-4 summarize the results for each solar sail configuration and for each load case. The data reported in these tables show that the boom in the MPCS model is less deflected and loaded in compression with respect to the 5PCS model. The differences introduced by the load incidence angles are quite small. The boom tip maximum deflection is always three order of magnitude smaller than the sail maximum deflection. Furthermore, the compression loads acting on the booms do not to cause problems of static resistance nor instability. Actually, the boom structural response should take into account its complex interaction with the deployment system, as is discussed in Ref. [29]. However, a detailed analysis focused on the boom structure is beyond the scope of this paper, which is focused on a technologically feasible design of the booms to describe the global structural response of the solar sail.

4.3. Vibration mode shapes and frequencies

For each configuration and load case, the first five non rigid-body vibration mode shapes and frequencies have been evaluated by means of the Lanczos algorithm, using an unsymmetrical solver. The eigenvectors have been normalized with the displacement. All of the modes calculated are membrane sail dominated and no disturbing

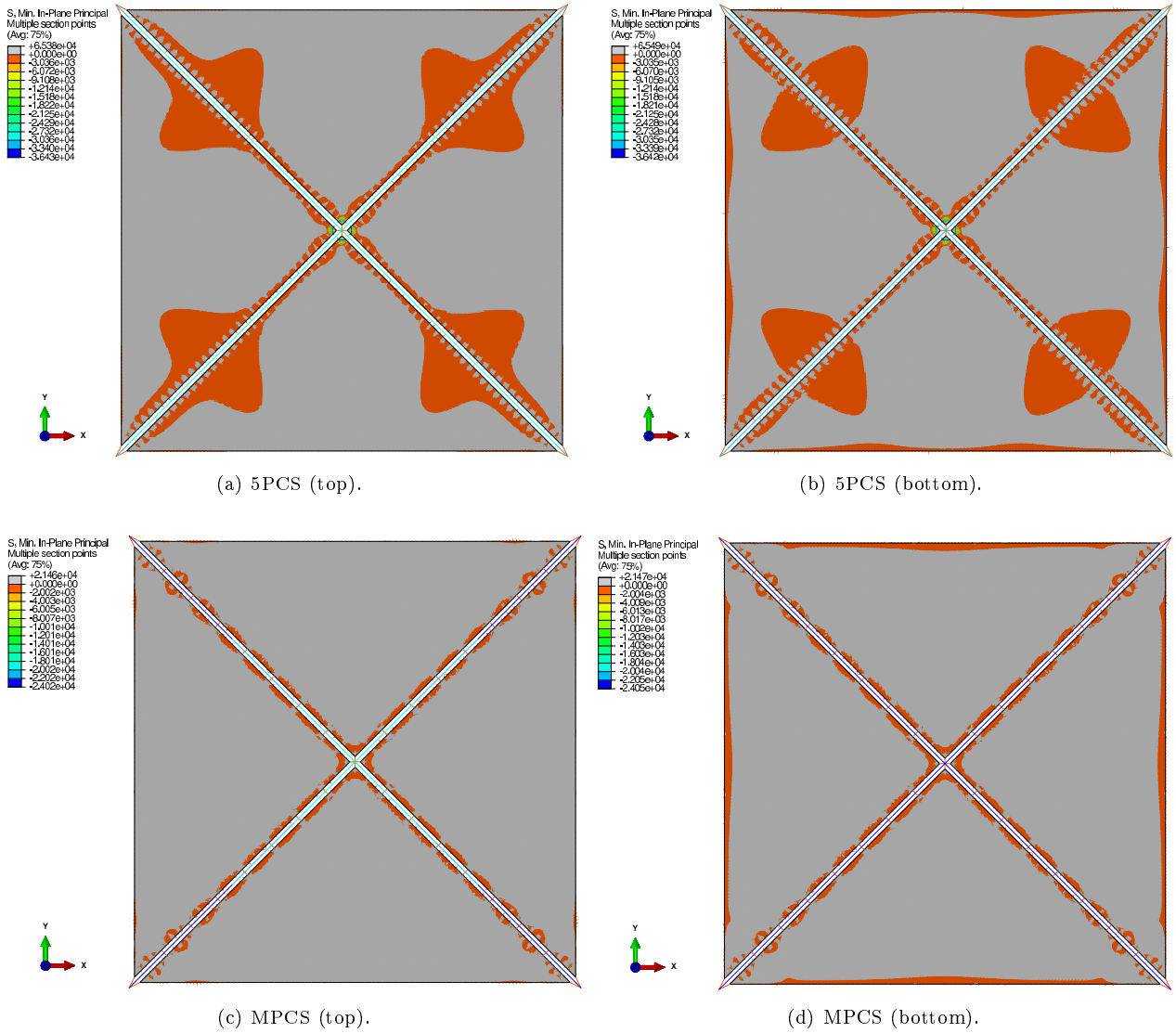


Figure 5. Minimum principal stress.

local mode has been found. This last result is consistent with the absence of large compressed regions in the sail surface. The mode shapes related to the normal pressure are shown in Fig. 6.

For non-zero off-normal and off-axis incidence angles, unsymmetrical mode shapes have been found, especially evident in the fifth mode. An example of this behavior is shown in Fig. 7 for the 5PCS model. Tables 5-6 summarize the value (used for displacement normalization) associated with the mode and the vibration frequencies for all of the analyzed cases. The mode frequencies of the MPCS configuration are always higher than those of the 5PCS. As far as the first four modes are concerned, the corresponding frequencies are closely spaced and do not exceed the value of 0.1 Hz for all configuration and load case. In particular, the second and third mode frequencies are coincident. The fifth mode frequency, especially in the 5PCS case, tends to move away from the previous ones, and is about 1 Hz.

Even though a direct comparison with other results from the literature is not a simple task, due to the differences existing in the solar sail size and configuration, and to the different loading conditions considered in the equilibrium reference state, nevertheless some general conclusions can be deduced. For example, the early

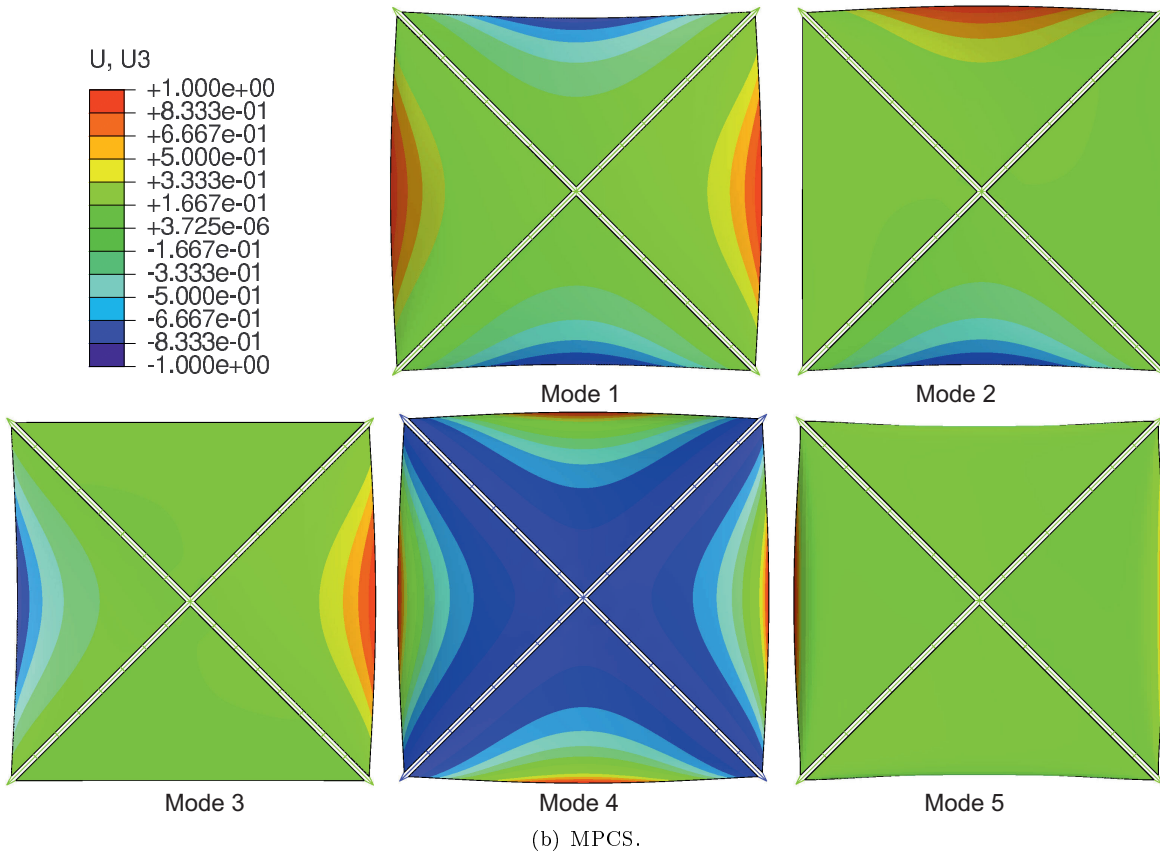
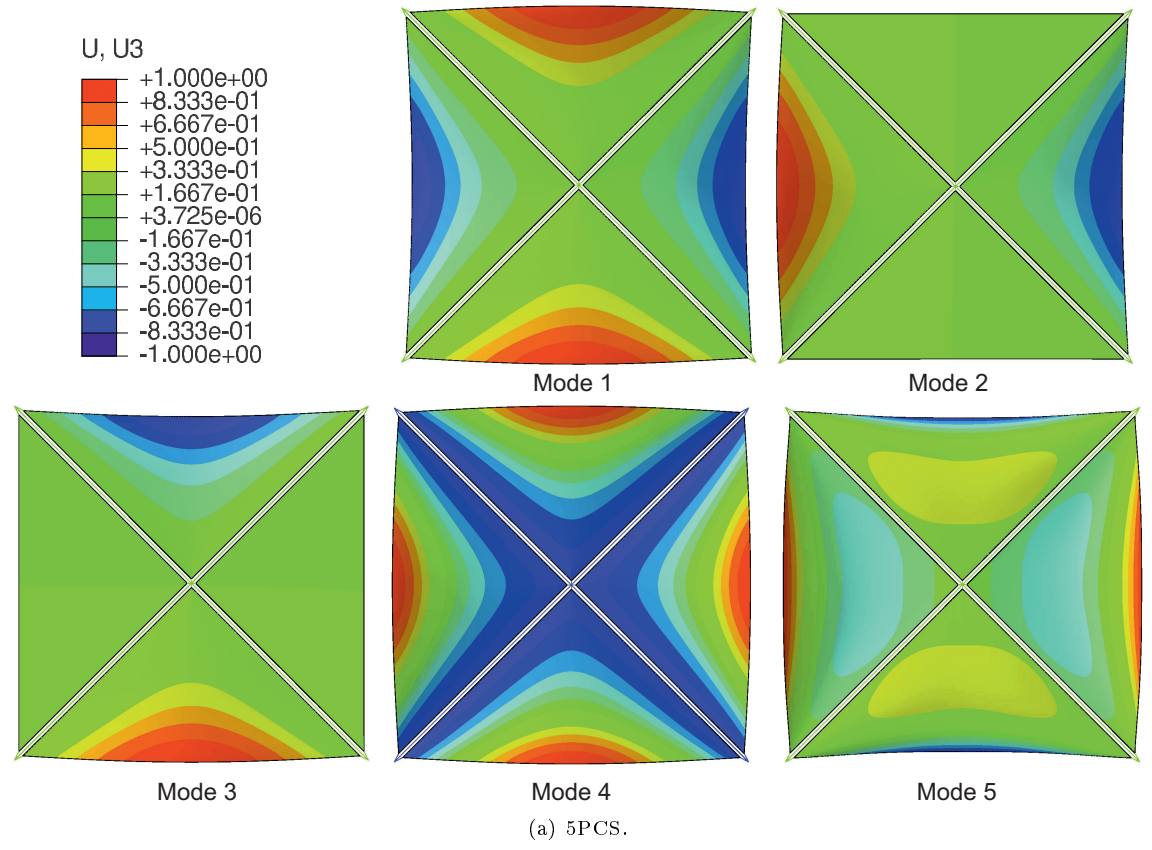


Figure 6. Vibration mode shapes.

Model	Angles					
	α	δ	α	δ	α	δ
	0	0	35 deg	0	35 deg	45 deg
5PCS	0.3315 N		0.3345 N		0.336 N	
MPCS	0.259 N		0.267 N		0.261 N	

Table 4. Maximum boom compression load as a function of the cone (α) and clock (δ) angle.

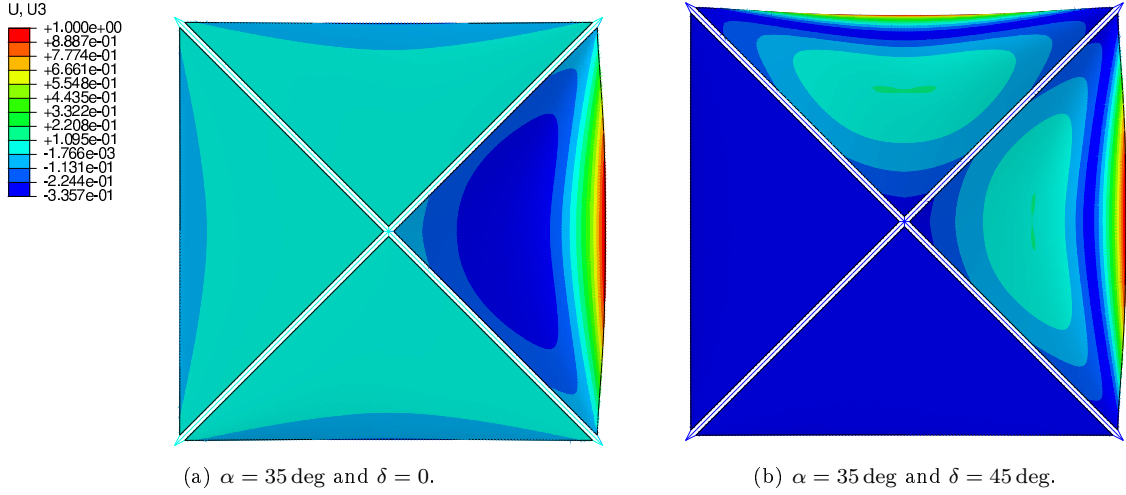


Figure 7. Fifth mode shape for the 5PCS model with non-zero incidence angles.

FE analyses²⁰, often provide the first mode shape and frequency only, with approximate information on the frequency range of the succeeding modes, the latter being usually well separated from the first one. In succeeding papers^{27,28,29}, the dynamic analysis aims at trying to reproduce the solar sail ground test conditions, which are actually much different from the free flying conditions considered in the present study. However, as is declared in Ref. [28], the FEA is able to correctly capture the mode frequencies and shapes only for solar sail configuration having boom-dominated modes, while the sail dominated modes does not correlate as well with experimental data. The results here presented are more comparable with those of Ref. [23], where similar conditions are considered for the non-linear equilibrium state, which are used to extract the vibration modes. In particular, the tendency of the first four modes frequencies to be closely spaced is confirmed. A closer comparison is prevented by the unrealistic mass distribution adopted in Ref. [23] for the small solar sail size and by the lack of results relevant to the MPCS configuration, whose modal analysis is confined to the calculation of the first mode only.

Model	5PCS			MPCS			
	Angles	$\alpha = \delta = 0$	$\alpha = 35$ deg, $\delta = 0$	$\alpha = 35$ deg, $\delta = 45$ deg	$\alpha = \delta = 0$	$\alpha = 35$ deg, $\delta = 0$	$\alpha = 35$ deg, $\delta = 45$ deg
Mode 1		0.17427	0.16861	0.16861	0.23821	0.22416	0.22416
Mode 2		0.17586	0.16969	0.16966	0.24475	0.22930	0.22931
Mode 3		0.17586	0.16969	0.16972	0.24475	0.22933	0.22932
Mode 4		0.18367	0.17481	0.17481	0.31580	0.28127	0.28126
Mode 5		0.42307	0.37463	0.37560	0.39991	0.35277	0.35325

Table 5. Vibration mode values.

Model	5PCS			MPCS		
	$\alpha = \delta = 0$	$\alpha = 35 \text{ deg}, \delta = 0$	$\alpha = 35 \text{ deg}, \delta = 45 \text{ deg}$	$\alpha = \delta = 0$	$\alpha = 35 \text{ deg}, \delta = 0$	$\alpha = 35 \text{ deg}, \delta = 45 \text{ deg}$
Mode 1	0.0664	0.0653	0.0656	0.0776	0.0753	0.0753
Mode 2	0.0667	0.0655	0.0655	0.0787	0.0762	0.0762
Mode 3	0.0667	0.0655	0.0655	0.0787	0.0762	0.0762
Mode 4	0.0682	0.0665	0.0665	0.0894	0.0844	0.0844
Mode 5	0.1035	0.0974	0.0975	0.1006	0.0945	0.0945

Table 6. Vibration mode frequencies (values in hertz).

5. Conclusions

The strategies adopted to perform the finite elements analysis detailed in this paper are well suited for collecting a large set of data that can be effectively used for a preliminary design of a square solar sail. The simulation results have been obtained by means of analysis techniques that considerably improve the methods currently available in the literature. The main characteristics of the proposed approach can be summarized in the following key points: the whole solar sail structure is studied in presence of distributed sail-boom connections; the inertia relief method is used to analyze a spacecraft in free flight at different incidence angles of the solar flux on the sail surface. As far as small solar sails are concerned, the convergence problems are solved by means of an effective sail pre-stress, the choice of an appropriate element type and a sufficient mesh refinement, without the need of any stabilization technique. However, the use of an initial geometrical imperfection on the whole solar sail geometry, perturbed with a suitable linear combination of the first global buckling modes, avoids the need of stabilization techniques also for larger solar sail sizes and improves the convergence performance. The global buckling modes are provided by a preliminary linear eigenvalue analysis, using an unsymmetrical eigensolver for the unsymmetrical loading conditions. As for the frequency analysis, the default symmetric eigensolver is replaced with an unsymmetrical one, which is able to correctly describe the vibration mode shapes and frequencies in presence of unsymmetrical loading conditions.

A detailed analysis has been performed on a reference $20 \text{ m} \times 20 \text{ m}$ solar sail. A comparison between the structural responses of the two analyzed configurations indicates higher performance of the multiple points connected sail with respect to the five points connected sail, with a negligible increment in total weight for the first configuration. As a matter of fact, the multiple connected sail results to be both less deformed and stressed, with a very low penalization in terms of sail loading. The presence of off-normal and off-axis incidence angles of the solar flux does not influence remarkably the stress-strain field of the solar sail. The performed study can be further improved by varying the materials and some geometrical characteristics of the solar sail components, such as the number of inner cables in the multiple points connected sail.

References

- [1] Tsuda Y., Mori O., Funase R., et al. : Achievement of IKAROS - Japanese Deep Space Solar Sail Demonstration Mission. In: Genta G, editor. Missions to the Outer Solar System and Beyond. Aosta, Italy: Seventh IAA Symposium on Realistic Near-Term Advanced Scientific Space Missions; 2011. .
- [2] Tsuda Y., Mori O., Funase R., et al. : Flight status of IKAROS deep space solar sail demonstrator. *Acta Astronautica*. 2011 November-December;69(9-10):833–840.
- [3] Mori O., Tsuda Y., Shirasawa Y., et al. : Attitude Control of IKAROS Solar Sail Spacecraft and Its Flight Results. In: 61st International Astronautical Congress. Prague, Czech Republic; 2010. Paper IAC-10.C1.4.3.

-
- [4] Johnson L., Whorton M., Heaton A., et al. : NanoSail-D: A solar sail demonstration mission. *Acta Astronautica*. 2011;68(5-6):571–575.
- [5] Johnson L., Young R., Barnes N., et al. : Solar sails: Technology and demonstration status. *International Journal of Aeronautical and Space Sciences*. 2012;13(4):421–427.
- [6] Johnson L., Young R., Montgomery E., et al. : Status of solar sail technology within NASA. *Advances in Space Research*. 2011;48(11):1687–1694.
- [7] Kezerashvili R. Y. : Solar sailing: Concepts, technology, and missions. *Advances in Space Research*. 2011;48(11):1683–1686.
- [8] Svitek T., Friedman L., Nye W., et al. : Voyage continues - LightSail-1 mission by the planetary society. In: 61st International Astronautical Congress. Prague, Czech Republic; 2010. p. 802–810.
- [9] McInnes C. R. : In: *Solar Sailing: Technology, Dynamics and Mission Applications*. Springer-Praxis Series in Space Science and Technology. Berlin: Springer-Verlag; 1999. p. 19–29.
- [10] McInnes C. R., Macdonald M., Angelopoulos V, et al. : GEOSAIL: Exploring the Geomagnetic Tail Using a Small Solar Sail. *Journal of Spacecraft and Rockets*. 2001 July-August;38(4):622–629.
- [11] Aliasi G., Mengali G., Quarta A. A. : Artificial Lagrange Points for Solar Sail with Electrochromic Material Panels. *Journal of Guidance, Control, and Dynamics*. 2013 September-October;36(5):1544–1550.
- [12] Mengali G., Quarta A. A. : Optimal heliostationary missions of high-performance sailcraft. *Acta Astronautica*. 2007 April-May;60(8-9):676–683.
- [13] Mengali G., Quarta A. A., Romagnoli D., et al. : H2-Reversal Trajectory: a New Mission Application for High-Performance Solar Sails. *Advances in Space Research*. 2011 December;48(11):1763–1777.
- [14] Macdonald M., editor. : *Advances in Solar Sailing*. Astronautical Engineering. Springer-Praxis; 2014. ISBN: 978-3-642-34906-5.
- [15] Ingrassia T., Faccin V., Bolle A., et al. : Solar sail elastic displacement effects on interplanetary trajectories. *Acta Astronautica*. 2013 February;82(2):263–272.
- [16] Peleri A., Barbera D., Laurenzi S., et al. : Dynamic and Structural Performances of a New Sailcraft Concept for Interplanetary Missions. *The Scientific World Journal*. 2015;2015. Article ID 714371.
- [17] Bolle A., Circi C. : Solar Sail Attitude Control Through In-Plane Moving Masses. *Proceedings of the Institution of Mechanical Engineers, Part G: Journal of Aerospace Engineering*. 2008 January;222(1):81–94.
- [18] Circi C. : Three-Axis Attitude Control Using Combined Gravity-Gradient and Solar Pressure. *Proceedings of the Institution of Mechanical Engineers, Part G: Journal of Aerospace Engineering*. 2007 January;221(1):85–90.
- [19] Greschik G., Mikulas M. M. : Design Study of a Square Solar Sail Architecture. *Journal of Spacecraft and Rockets*. 2002 September-October;39(5):653–661.
- [20] Murphy D., Murphey T., Gierow P. : Scalable Solar Sail Subsystem Design Considerations. In: 43rd AIAA/ASME/ASCE/AHS/ASC Structures, Structural Dynamics, and Materials Conference. Denver, CO; 2002. Paper AIAA-2002-1703.
- [21] Wong Y., Pellegrino S. : Prediction of Wrinkle Amplitudes in Square Solar Sails. In: 44th AIAA/ASME/ASCE/AHS/ASC Structures, Structural Dynamics, and Materials Conference. Norfolk, Virginia; 2003. Paper AIAA 2003-1982.
- [22] Su X., Abdi F., Taleghani B., et al. : Wrinkling Analysis of a Kaptan Square Membrane under Tensile Loading. In: 44th AIAA/ASME/ASCE/AHS Structures, Structural Dynamics, and Materials Conference. Norfolk, Virginia; 2003. Paper AIAA 2004-1509.
- [23] Sleight D., Muheim D. : Parametric Studies of Square Solar Sails Using Finite Element Analysis. In: 45th AIAA/ASME/ASCE/AHS/ASC Structures, Structural Dynamics & Materials Conference. Palm Springs, California; 2004. Paper AIAA 2004-1509.
- [24] Liao L. : A Study of Inertia Relief Analysis. In: 52nd AIAA/ASME/ASCE/AHS/ASC Structures, Structural Dynamics and Materials Conference. Denver, Colorado; 2011. Paper AIAA 2011-2002.

- [25] Potes F. C. : General conceptual design problems of a parabolic solar sail structure. Universidade da Beira Interior; 2012.
- [26] Herbeck L., Sickinger C., Eiden M., et al. : Solar Sail hardware Developments. In: European Conference on Spacecraft Structures, Materials and Mechanical Testing. Toulouse, France; 2002. .
- [27] Taleghani B., Lively P., Gaspar J., et al. : Dynamic and Static Shape Test/analysis Correlation of a 10 Meter Quadrant Solar Sail. In: 46th AIAA/ASME/ASCE/AHS/ASC Structures, Structural Dynamics and Materials Conference. Austin, Texas; 2005. Paper AIAA 2005-2123.
- [28] Taleghani B., Lively P., Banik J., et al. : 20 Meter Solar Sail Analysis and Correlation. In: Joint Army Navy Nasa Air Force (JANNAF) Meeting. Monterey, CA; 2005. Paper TTA M-ISP-03-23.
- [29] Sleight D., Michii Y., Lichodziejewski D., et al. : Structural Analysis of an Inflation-Deployed Solar Sail with Experimental Validation. In: 41st AIAA/ASME/SAE/ASEE Joint Propulsion Conference & Exhibit. Tucson, Arizona; 2005. Paper AIAA 2005-3727.
- [30] Banik J., Lively P., Taleghani B., et al. : Solar Sail Topology Variations Due to On-Orbit Thermal Effects. In: 47th AIAA/ASME/ASCE/AHS/ASC Structures, Structural Dynamics, and Materials Conference. Newport, Rhode Island; 2006. Paper AIAA 2006-1708.
- [31] Sakamoto H., Park K. C., Miyazaki Y. : Effect of Static and Dynamic Solar Sail Deformation on Center of Pressure and Thrust Forces. In: AIAA Guidance, Navigation, and Control Conference and Exhibit. Keystone, Colorado; 2006. Paper AIAA 2006-6184.
- [32] Holland D. B. : Static and dynamic characteristics of end-loaded beams with specific application in square solar sails. Duke University; 2007. ISBN: 9780549662136.
- [33] Anon. : Abaqus 6.11 Analysis User's Manual - Volume II: Analysis; 2011.
- [34] Boni L., Fanteria D., Lanciotti A. : Post-buckling behaviour of flat stiffened composite panels: Experiments vs. analysis. Composite Structures. 2012 December;94(12):3421–3433.
- [35] Liu J., Cui N., Shen F., et al. : Dynamics of highly-flexible solar sail subjected to various forces. Acta Astronautica. 2014;103:55–72.
- [36] Jenkins C. H. M., editor. : Gossamer Spacecraft: Membrane and Inflatable Structures Technology For Space Applications. vol. 191 of Progress in Astronautics and Aeronautics. American Institute of Aeronautics and Astronautics; 2001. ISBN: 978-1-56347-403-3.